Macromolecular Bioscience
www.mbs-journal.de

Photo- and pH-Responsive Polycarbonate Block Copolymer Prodrug Nanomicelles for Controlled Release of Doxorubicin

*Nagendra Kalva, Saji Uthaman, Rimesh Augustine, Su Hyeon Jeon, Kang Moo Huh, In-Kyu Park, and Il Kim**

Photo/pH dual-responsive amphiphilic diblock copolymers with alkyne functionalized pendant *o*-nitrobenzyl ester group are synthesized using poly(ethylene glycol) as a macroinitiator. The pendant alkynes are functionalized as aldehyde groups by the azide-alkyne Huisgen cycloaddition. The anticancer drug doxorubicin (DOX) molecules are then covalently conjugated through acid-sensitive Schiff-base linkage. The resultant prodrug copolymers self-assemble into nanomicelles in aqueous solution. The prodrug nanomicelles have a well-defined morphology with an average size of 20–40 nm. The dual-stimuli are applied individually or simultaneously to study the release behavior of DOX. Under UV light irradiation, nanomicelles are disassembled due to the ONB ester photocleavage. The light-controlled DOX release behavior is demonstrated using fluorescence spectroscopy. Due to the pH-sensitive imine linkage the DOX molecules are released rapidly from the nanomicelles at the acidic pH of 5.0, whereas only minimal amount of DOX molecules is released at the pH of 7.4. The DOX release rate is tunable by applying the dual-stimuli simultaneously. In vitro studies against colon cancer cells demonstrate that the nanomicelles show the efficient cellular uptake and the intracellular DOX release, indicating that the newly designed copolymers with dual-stimuli-response have significant potential applications as a smart nanomedicine against cancer.

1. Introduction

Nanomedicine is one of the powerful therapeutic strategy to treat cancer, which can deliver the anticancer drugs precisely to tumor site by enhanced permeation and retention effect (EPR).[1,2] In order to improve therapeutic efficiency and reduce the side effects of these drugs, several drug delivery systems such as polymer micelles,[3–9] inorganic nanoparticles,[10–14] liposomes,[15,16] dendrimers,[17–20] and polymer-prodrug conjugates[21–30] have been developed as nanomedicines.

Particularly amphiphilic block polymer nanocarriers have been developed to improve the anticancer efficiency by utilizing their prolonged circulation time, improved solubility of the hydrophobic drugs and reduced side effects.[31,32] However, their clinical use is hampered by the premature drug release during the process of blood circulation, leading to reduced drug accumulation at the target-site. The polymer prodrugs are considered as a candidate to overcome these obstacles, where the anticancer drugs are covalently attached to the polymer backbone and side chains through stimuli-responsive linkers that can be cleaved in different stimuli conditions. Polymer prodrug nanoparticles are featured by their unique properties such as high stability over physiological conditions and improved drug loading.[33,34]

Stimuli-responsive polymer prodrugs have been widely studied with physiological environmental changes such as pH, temperature, redox environment, and specific enzymes. Among this pH-responsive polymer prodrug scaffolds attracted a lot of interest due to the presence of pH gradient between healthy and tumor cells. For example, acidic pH microenvironment found at the tumor cells such as extracellular matrix (pH 6.5–7.2) and endosomes (pH 5.0–6.5). Many types of acid cleavable linkages are incorporated in the polymer prodrug conjugates such as hydrazone, acetal, ketal, Schiff base, and β-thioester that are cleaved under mild acidic conditions.[25,26,28,35] Many examples have also been demonstrated the incorporation of photo-cleavable groups into the main or side chain of the polymers.[36–40] Among many photo-cleavable groups *o*-nitrobenzyl (ONB)

Dr. N. Kalva, R. Augustine, S. H. Jeon, Prof. I. Kim
BK21 PLUS Centre for Advanced Chemical Technology
Department of Polymer Science and Engineering
Pusan National University
Busan 46241, Republic of Korea
E-mail: ilkim@pusan.ac.kr
Dr. S. Uthaman, Prof. K. M. Huh
Department of Polymer Science and Engineering
Chungnam National University
Daejeon 34134, Republic of Korea
Prof. I.-K. Park
Department of Biomedical Science
BK21 PLUS Centre for Creative Biomedical Scientists
Chonnam National University Medical School
Gwangju 61469, Republic of Korea
The ORCID identification number(s) for the author(s) of this article can be found under https://doi.org/10.1002/mabi.202000118.

DOI: 10.1002/mabi.202000118

alcohol derivatives gained considerable attention since light provides remote and spatiotemporal control by tuning the wavelength, energy, and irradiation site. ONB esters are efficiently cleaved under UV light irradiation to yield carboxylic acids.[41,42]

Polycarbonate (PC) presents excellent biocompatibility, biodegradability, and low toxicity. PC can be functionalized with various functional groups for specific theranostic applications.[43–45] Organocatalytic ring-opening polymerization (ROP) has been developed for the synthesis of various functional PCs for drug and gene delivery applications.[46–49] For example, the photo-responsive PC diblock copolymers with spiropyran chromophore in the side chain showed a reversible micelle transition in aqueous solution due to the photoisomerization between spiropyran (SP) and merocyanine (MC) form.[50] The pH/redox dual-responsive PC diblock copolymers functionalized with disulfide bonds and pH-responsive carboxylic acid groups[51] and the photo-responsive PC diblock copolymers functionalized with ONB ester[36] were synthesized by employing the ROP. The resultant photo-responsive micelles were disassembled upon UV irradiation and released a model hydrophobic dye Nile red. The triple-stimuli-responsive PCs with temperature-, redox-, and light-responsive groups in the backbone as well as side chain of the polymer were recently reported.[52] Even though some different strategies have been reported for the synthesis of photo-responsive polymers with ONB esters, there have been few reports on the stimuli-responsive nanomedicines fabricated by using PCs functionalized with light-responsive ONB ester group.

In this study, we have synthesized two amphiphilic diblock PCs with photo- and pH-cleavable linkers in the side chain. Photo-cleavable alkyne-functionalized ONB ester was introduced to the cyclic carbonate. PCs were then synthesized via an organocatalytic ROP of 2,2,5-trimethyl-1,3-dioxane-5-carboxylate bearing pendant propargyl-substituted ONB ester (TMDC–ONB) using monomethylether poly(ethylene glycol) (mPEG) as a macroinitiator. The pendant alkyne groups in ONB moieties were transformed to aldehyde groups by azide–alkyne click reaction. Anticancer drug doxorubicin (DOX) was then covalently conjugated to the polymers via a pH-sensitive Schiff base linkage. The structures of the resulting polymer prodrugs were characterized by spectroscopic analysis and gel permeation chromatography (GPC). The resultant photo- and pH-dual-stimuli-responsive prodrugs self-assembled into spherical NMs in aqueous solution. In vitro drug release behavior of the prodrug nanomicelles (NMs) at different pH- and photo-stimuli was investigated. The cellular uptake and in vitro antitumor activity of DOX-conjugated NMs were also investigated in colon cancer cells (CT26).

2. Experimental Section

2.1. Materials

2,2-bis-methylolpropionic acid (bis-MPA), anhydrous *N,N*-dimethylformamide (DMF), 2,2-dimethoxypropane, 5-hydroxy-2-nitrobenzaldehyde, poly(ethylene glycol) monomethyl ether (mPEG; molecular weight (M_W) = 2000 and 5000), sodium borohydride were purchased from Sigma-Aldrich Korea and used without further purification. Propargyl bromide, 4-dimethylaminopyridine (DMAP), pyridine, copper(I) iodide, *p*-toluene sulfonyl chloride, triethyl amine, potassium carbonate, ethyl chloroformate, 1-chlorohexanol, sodium azide, dicyclohexylcarbodiimide (DCC), 1,8-diazabicyclo [5.4.0] undec-7-ene (DBU), 4-formyl benzoic acid, and triethylamine were purchased from Acros Organics Company (New Jersey, USA). 5-Propargylether-2-nitrobenzyl alcohol,[53] bis-MPA anhydride,[54] tris[(1-benzyl-1*H*-1,2,3-triazol-4-yl)methyl]amine (TBTA),[55] and 6-azidohexyl 4-formylbenzoate[23] were synthesized as per reported procedures. Dichloromethane (DCM) was dried over CaH_2 distilled and stored in Schlenk flask. Tetrahydrofuran (THF) was passed through alumina, dried on sodium wire, and freshly distilled when required. Common solvents like hexane, ethyl acetate, dichloromethane, and methanol were purchased from Duksan Chem. Co. (Daejeon, Korea) and distilled prior to use.

2.2. Instrumentation

^{1}H NMR (400 MHz) and ^{13}C NMR (100 MHz) spectra were recorded using a Varian INOVA 400 NMR spectrometer with tetramethylsilane (TMS) as the internal standard. GPC system using THF an eluent at a flow rate of 1.0 mL min^{-1} and calibrated with monodisperse polystyrene used to measure the average molecular weights (M_W) and polydispersity index ($Đ$). UV–vis spectra were recorded using a Shimadzu UV-1650 PC. A Shimadzu IR Prestige 21 spectrometer was used to record the FTIR spectra using potassium bromide discs in the range of 4000–600 cm^{-1}. The dynamic light scattering (DLS) for the particle size measurement was performed using a Nano ZS90 zeta potential analyzer (Malvern Instruments, UK) with a He–Ne laser (633 nm), 90° collecting optics and a thermoelectric Peltier temperature controller. The particle morphology was analyzed using transmission electron microscopy (TEM) with a JEOL-1299EX electron microscope at an accelerating voltage of 80 keV. The TEM samples were prepared in grids with formvar film and treated with oxygen plasma (from a Harrick plasma cleaner/sterilizer) for 15 s to render the surface hydrophilic.

2.3. Synthesis of 5-Hydroxy 2-nitrobenzyl Alcohol

In a round bottom flask, 5-hydroxy-2-nitrobenzaldehyde (3.5 g, 20.9 mmol) was dissolved in dry methanol and cooled the solution to 0 °C using an ice bath. Sodium borohydride ($NaBH_4$) (1.76 g, 46.5 mmol) was slowly added to this solution under nitrogen flow at 0 °C. The resulting solution allowed to room temperature by removing an ice bath and stirred for additional 3 h. The mixture was quenched carefully using aqueous HCl solution (10 vol%) and the solvent was removed under reduced pressure using a rotary evaporator. The reaction mixture was extracted with ethyl acetate and washed with brine solution. The organic layer was dried with sodium sulfate and was concentrated under reduced pressure. The crude mixture was purified using column chromatography by eluting with ethyl acetate and petroleum ether (1:1 v/v) to obtain yellow solid (yield = 90%). ^{1}H NMR (CD_3OD, 400 MHz) 4.81(s, 2H), 5.62(bs, 1H), 6.77(dd, 8 Hz, 1H), 7.23(s, 1H), 8.03(d, J = 16 Hz, 1H) ppm. ^{13}C NMR (CD_3OD, 100 MHz): 163.07, 141.84, 138.63, 127.44, 113.64, 60.94 ppm.

2.4. Synthesis of 5-Propargylether-2-nitrobenzyl Alcohol 1

5-hydroxy 2-nitro benzyl alcohol (2.3 g, 13.6 mmol) and potassium carbonate (5.63 g, 40.7 mmol) were dissolved in dry dimethylformamide and stir for one hour at 60 °C. Propargyl bromide (80% in toluene), was added drop by drop and the mixture was stir for 24 h at 60 °C. After completion of the reaction, DMF was removed under reduced pressure. The reaction mixture was extracted into ethyl acetate and washed with water. The organic phase dried with sodium sulfate and the solvent was removed under reduced pressure. The crude yellow solid purified by the column chromatography eluting with 20% ethyl acetate and petroleum ether to get yellow fluffy solid (yield = 85%). ^{1}H NMR (CD_3OD, 400 MHz): 3.06(d, J = 12 Hz, 2H), 4.91(d, J = 4 Hz, 2H), 5.00(s, 2H), 7.06(dd, 8 Hz, 1H), 7.49(s, 1H), 8.17(d, J = 8 Hz, 1H) ppm. ^{13}C NMR (CD_3OD, 100 MHz): 56.43, 61.69, 77.48, 113.63, 113.95, 127.75, 140.52, 142.08, 162.33 ppm.

2.5. Synthesis of Compound 2

Compound **1** (1.5 g, 7.2 mmol), bis-MPA anhydride (3.5 g, 10.6 mmol), DMAP (0.14 g, 1.1 mmol), and pyridine (1.16 mL, 14.4 mmol) were added to dry CH_2Cl_2 in a reaction flask under argon flow and reaction mixture was stirred at room temperature for 15 h. After completion, the reaction excess anhydride was quenched carefully with the addition of 2 mL of water under vigorous stirring, followed of dilution with 300 mL of CH_2Cl_2 and the solution was washed with 10 % of $NaHSO_4$ (3 × 500 mL), and 10 % of Na_2CO_3 (3 × 500 mL). The organic phase dried over Na_2SO_4, concentrated and purified by column chromatography on silica gel, eluting with hexane and gradually increasing the polarity to ethyl acetate and petroleum ether (30:70) to give yellow solid (yield = 92%). ^{1}H NMR ($CDCl_3$, 400 MHz): 1.20(s, 3H), 1.40(s, 3H), 1.46(s, 3H), 2.56(t, J = 4 Hz, 1H), 3.71(d, J = 12 Hz, 2H), 4.28(d, J = 12 Hz, 2H), 4.79(d, J = 4 Hz, 2H), 5.65(s, 2H), 6.98(dd, 8 Hz, 1H), 7.27(s, 1H), 8.19(d, J = 12 Hz, 1H) ppm. ^{13}C NMR ($CDCl_3$, 100 MHz): 18.57, 21.25, 26.37, 42.49, 56.39, 63.56, 66.35, 98.45, 113.90, 114.33, 127.97, 135.94, 140.73, 161.90, 173.71 ppm.

2.6. Synthesis of Compound 3

Compound **2** (3.5 g, 9.6 mmol) was dissolved in 15 mL THF and 15 mL of 1 N HCl was added and stirred overnight at room temperature. The reaction monitored by the TLC after completion of the reaction, the reaction mixture was diluted with 100 mL DCM and wash three times with 0.1 M sodium carbonate solution and twice with brine solution. The crude product was purified by eluting with ethyl acetate and petroleum ether (40:60) to obtain white solid (yield = 85%). ^{1}H NMR (CD_3OD, 400 MHz): 1.23(s, 3H), 3.04(t, J = 4 Hz, 1H), 3.67(d, J = 12 Hz, 2H), 3.78(d, J = 12 Hz, 2H), 4.88 (d, J = 4 Hz, 2H), 5.56(s, 2H), 7.06(dd, 8 Hz, 1H), 7.34(d, J = 4 Hz, 1H), 8.17(d, J = 8 Hz, 1H) ppm. ^{13}C NMR (CD_3OD, 100 MHz): 16.04, 50.62, 55.63, 62.91, 64.63, 76.48, 77.29, 113.37, 114.21, 127.20, 135.63, 140.41, 161.90, 174.65 ppm.

2.7. Synthesis of 2,2,5-Trimethyl-1,3-dioxane-5-carboxylate with TMDC-ONB

Compound **3** (1 g, 3.2 mmol) was dissolved in dry 20 mL THF and ethyl chloroformate (1.23 mL, 12.8 mmol) was added drop by drop and was stirred at room temperature. The reaction mixture cool to 0 °C and stir for 30 min. Then add triethylamine (1.81 mL, 12.8 mmol) drop by drop over 30 min and stir at 0 °C for another 2 h. The reaction mixture was allowed to the room temperature and stir overnight. After completion of the reaction filter triethylamine salts using a sintered funnel and remove THF under reduced pressure. The reaction mixture was dissolved in DCM and purified by column chromatography eluting with ethyl acetate and dichloromethane (20:80) to yield white solid (yield = 70%). ^{1}H NMR (DMSO-D_6, 400 MHz): 1.26 (s, 3H), 3.78(t, J = 4 Hz, 1H), 4.41(d, J = 12 Hz, 2H), 4.63 (d, J = 12 Hz, 2H), 5.01(d, J = 4 Hz, 2H), 5.57(s, 2H), 7.18-7.23(m, 2H), 8.21(d, J = 12 Hz, 1H) ppm. ^{13}C NMR (DMSO-D_6, 100 MHz): 16.61, 56.57, 64.28, 72.69, 78.44, 79.54, 114.75, 115.10, 128.16, 134.35, 140.67, 147.42, 161.59, 171.47 ppm.

2.8. General Procedure for the Synthesis of Diblock Copolymers P1 and P2

The commercially available mPEG was used as a macroinitiator for the ring-opening polymerization. The polymerization was conducted under N_2 inert atmosphere and using Schlenk line technique. For example, mPEG (M_W = 5000) (0.4 g, 0.08 mmol) and TMDC-ONB (0.558 g, 3.6 mmol) were placed in a dried Schlenk tube and were dissolved in dry DCM. The mixture was purged 30 min to remove the trace moisture and oxygen. The DBU catalyst (0.01 g, 0.065 mmol) was then added to start the polymerization at 30 °C. After stirring at room temperature for 6 h, the resulting reaction mixture was precipitated in cold ether and purified by using a small plug of silica column by eluting with 5% methanol and dichloromethane to obtain white solid P1 (0.65 g; yield = 88%). P2 was prepared in the same procedure using mPEG (M_W = 2000).

P1: ^{1}H NMR ($CDCl_3$, 400 MHz): 1.26 (s $-CCH_3$), 2.62 (t, J = 4 Hz, 1H), 3.37 (s, 3H, $-OCH_3$) 3.63 (s, $-OCH_2CH_2-$), 4.33 (dd, J = 12 Hz, $-CCH_2-O-$), 4.79 (s, $-OCH_2-$), 5.51 (s, $-ArCH_2-$, 2H), 6.97–7.07 (m, aromatic), 8.21(d, J = 12 Hz, aromatic) ppm. M_n = 10.2 kDa and $Đ$ = 1.10.

P2: ^{1}H NMR ($CDCl_3$, 400 MHz): 1.27 (s $-CCH_3$), 2.63 (t, J = 4 Hz, 1H), 3.37 (s, 3H, $-OCH_3$) 3.63 (s, $-OCH_2CH_2-$), 4.35 (dd, J = 12 Hz, $-CCH_2-O-$), 4.80 (s, $-OCH_2-$), 5.58 (s, $-ArCH_2-$, 2H), 7.00–7.16 (m, aromatic), 8.17(d, J = 12 Hz, aromatic) ppm. M_n = 5.1 kDa and $Đ$ = 1.13.

2.9. Synthesis of Aldehyde Functionalized P1–CHO and P2–CHO by Click Reaction

P1 (0.4 g, 0.038 mmol) and 6-azidohexyl 4-formylbenzoate (0.169 g, 0.6 mmol) were dissolved in THF and purged with nitrogen gas for 30 min. In another vial TBTA (0.024 g, 0.047 mmol) was dissolved in THF and purged with N_2 gas for 10 min. To this solution Cu(1)I (0.008 g, 0.042 mmol) was added

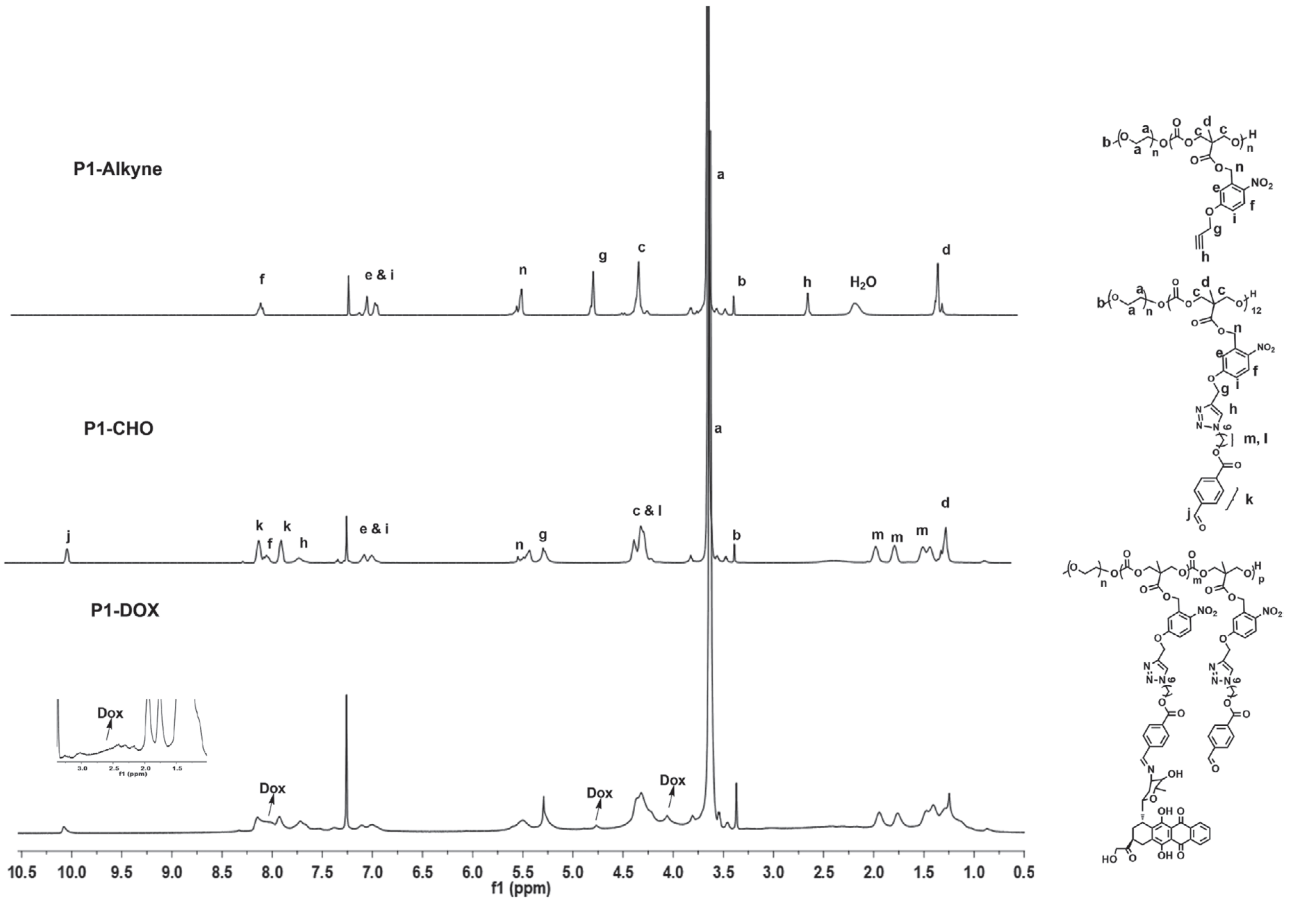

Figure 1. ^{1}H NMR spectra of P1 (top), P1–CHO (middle) and P1–DOX (bottom) in $CDCl_3$.

and purged for an additional 15 min. This catalytic solution was then added to the above reaction mixture and stirred for 24 h at room temperature. The resultant reaction mixture was precipitated in diethyl ether to obtain pure white solid P1–CHO (yield = 85%). P2–CHO was prepared in the same way using P2.

P1–CHO (**Figure 1**): ^{1}H NMR ($CDCl_3$, 400 MHz): 1.24 (s $-CCH_3$), 1.41–1.47 (m $-CH_2CH_2-$), 1.76 (s, $-OCH_2CH_2-$), 1.95 (s, $-NCH_2-$), 3.37 (s, 3H, $-OCH_3$) 3.63 (s, $-OCH_2CH_2-$ for PEG), 4.31–4.37 (m, $-CCH_2-O-$ and $-COO-CH_2-$), 5.29 (s, $-OCH_2-$), 5.42 (s, $-ArCH_2-$, 2H), 7.01–7.08 (m, aromatic), 7.74 (s, triazole proton), 7.92 (s, aromatic), 8.06–8.14(m, aromatic), 10.06 (s, 1H proton from $-$ArCHO) ppm.

P2–CHO (Figure S14, Supporting Information): ^{1}H NMR ($CDCl_3$, 400 MHz): 1.25 (s $-CCH_3$), 1.40–1.48 (m $-CH_2CH_2-$), 1.78 (s, $-OCH_2CH_2-$), 1.96 (s, $-NCH_2-$), 3.37 (s, 3H, $-OCH_3$) 3.63 (s, $-OCH_2CH_2-$ for PEG), 4.26–4.38 (m, $-CCH_2-O-$ and $-COO-CH_2-$), 5.30 (s, $-OCH_2-$), 5.54 (s, $-ArCH_2-$, 2H), 7.00–7.11 (m, aromatic), 7.70 (s, triazole proton), 7.93 (s, aromatic), 8.10–8.16 (m, aromatic), 10.08 (s, 1H proton from –ArCHO) ppm.

2.10. Synthesis of Prodrug Polymers P1–DOX and P2–DOX

DOX·HCl (50 mg) was dissolved in 1 mL of DMSO and added two equivalents of TEA (24 µL) to neutralize HCl. The mixture was stirred in dark for 2 h and then added to the solution of P1–CHO (50 mg) or P2–CHO (50 mg) in 1 mL of DMSO. After stirring reaction mixture for 48 h, the product was dialyzed against deionized water using dialysis membrane with molecular weight cut-off (MWCO) of 3.5 kDa for 4 d to remove DMSO and unreacted DOX. The resultant solution was freeze-dried to obtain magenta red DOX-conjugated polymers. The DOX content was determined by measuring fluorescence in DMSO at 480 nm. A standard curve was constructed to measure DOX concentration in the solution.

P1–DOX (Figure 1): ^{1}H NMR ($CDCl_3$, 400 MHz): 0.87–1.95(br m, all $-CH_3$ protons from 4 and 8H from 5 ($-NCH_2(CH_2)_4-CH_2-$); 5H from DOX ($-CHCH_2$ and $-CH_3$), 2.0–2.41 (br m, 2H from DOX), 2.94–3.0 (br m, 2H from DOX $ArCH_2C-$), 3.37 (s, 3H, $-OCH_3$) 3.63 (s, $-OCH_2CH_2-$ for PEG), 3.90-4.60 (brm, $-CCH_2-O-$ and $-COO-CH_2-$, and 2H from DOX $-COCH_2OH$), 4.76(s, 2H from DOX), 5.29 (s, $-OCH_2-$), 5.42 (s, $-ArCH_2-$, 2H), 7.01–7.08 (m, aromatic), 7.30–8.37(br m, ArH from 5 and DOX, and 1H, from triazole), 10.06 (s, 1H proton from $-$ArCHO) ppm. M_n = 18.0 kDa and $Đ$ = 1.13.

P2–DOX (Figure S15, Supporting Information): ^{1}H NMR ($CDCl_3$, 400 MHz): 0.83-1.95(br m, all $-CH_3$ protons from 4 and 8H from 5 ($-NCH_2(CH_2)_4-CH_2-$); 5H from DOX ($-CHCH_2$ and $-CH_3$), 2.0–2.41 (br m, 2H from DOX), 2.94–3.0 (br m, 2H from DOX $ArCH_2C-$), 3.37 (s, 3H, $-OCH_3$)

3.63 (s, $-OCH_2CH_2-$ for PEG), 3.96–4.66 (m, $-CCH_2-O-$ and $-COO-CH_2-$ and 2H from DOX $-COCH_2OH$), 4.77(s, 2H from DOX), 5.29 (s, $-OCH_2-$), 5.42 (s, $-ArCH_2-$, 2H), 7.01–7.08 (m, aromatic), 7.35–8.39 (br m, ArH from 5 and DOX, and 1H from triazole), 10.08 (s, 1H proton from −ArCHO) ppm. M_n = 10.0 kDa and $Đ$ = 1.15.

2.11. Preparation of Aqueous Solution of Prodrug NMs and Characterization

The NMs of P1–DOX or P2–DOX prodrugs were fabricated by solvent exchange method. 10 mg of the amphiphilic prodrug polymers were dissolved in 2 mL of THF at room temperature. Deionized water was then added drop by drop with vigorous stirring to get the final concentration of 1 mg mL^{-1}. After stirring the solution at room temperature for 2 h, placed the solution into a dialysis bag (MWCO 3.5 kDa) and dialyzed against water for 2 days to remove THF.

2.12. CMC Measurements

Nile Red stock solution (5×10^{-6} M) was prepared and added to the empty vials to make nile red film on the glass walls. The aqueous solution of the polymer (1 mg mL^{-1}) was added to the above vial and diluted by the addition of water to get series of concentrations and allowed to encapsulate Nile Red in the micelle core at room temperature. Fluorescence emission spectra of Nile Red in aqueous solutions were recorded and constructed a plot of intensity versus log(concentration). CMC was determined to be the point where the two tangents to the curve crossed.

2.13. In Vitro DOX Release

The in vitro DOX release from the P1–DOX and P2–DOX prodrug NMs were investigated at a concentration of 2 mg mL^{-1} in the presence of three types of phosphate buffer solutions with different pHs, pH 7.4, pH 6.0, and pH 5.0, respectively. 2 mL aqueous solutions of the NMs were placed in a dialysis membrane (MWCO 3.5 kDa) and then all the dialysis tubes were immersed in 15 mL of phosphate buffer solution. All the tubes were placed in a water bath at 37 °C under gentle shaking in a dark environment. One milliliter of the external solution was taken out and replenished with 1.0 mL of fresh PBS solution. The concentration of the DOX was determined by fluorescence spectrophotometer under excitation at 480 nm and emission at 550 nm with a slit width set as 5 nm. All the results were measured in triplicate.

2.14. Cellular Viability

In order to investigate the cellular viability of P1–DOX and P2–DOX on cancer cell line, the water-soluble tetrazolium (WST-1) assay was performed. Briefly, 1×10^4 cells per well were seeded and cultured overnight in 96-well plate in optimum culturing conditions (37 °C and 5% CO_2). After overnight culturing, the media was aspirated and fresh media containing various concentrations of P1–DOX and P2–DOX were supplemented and cells were further incubated for 24 h. The media was then removed and cells were washed with 1 × dulbecco's phosphate-buffered saline (DPBS) and 0.1 mL of fresh media was added. After which WST-1 assay was performed as per the manufacture's protocol.

2.15. Cellular Uptake and Fluorescence-Activated Cell Sorting Analysis

In order to understand the intercellular uptake potential of P1–DOX, confocal microscopy and fluorescence-activated cell sorting (FACS) analysis were performed. Briefly, for confocal microscopy, CT26 cells were cultured overnight in Lab-Tek Chamber Slide with a seeding density of 1×10^4 cells per well. After overnight incubation, media was removed, P1–DOX and DOX in cell culture media (DOX concentration = 10 mg mL^{-1}) were added to the cells and further incubated for 6 h. The media was then removed and washed with 1 × PBS for three times. The cells were fixed by the addition of 4% paraformaldehyde and the nucleus was stained with 4′,6-diamidino-2-phenylindole (DAPI). Confocal microscopy was used for visualizing the DOX fluorescence. For FACS analysis 1×10^6 cells per well were seeded in six-well plate and cultured overnight. The media was then aspirated and samples were added at a DOX concentration of 10 mg mL^{-1} and incubated for 6 h. After incubation, media was removed and cells were washed with 1 × PBS for three times. The cells were then suspended in FACS buffer and subjected to FACS analysis.

3. Results and Discussion

3.1. Synthesis and Characterization of Monomer and Polymers

The TMDC-ONB monomer bearing pendant propargyl-substituted ONB ester was synthesized via three steps as illustrated in **Scheme 1**. The structure was confirmed by using ^{1}H NMR and ^{13}C NMR spectroscopy (Figures S1–S10, Supporting Information (SI)). The diblock polycarbonates P1 and P2 were synthesized via an organocatalytic ring-opening polymerization (ROP) of cyclic carbonate monomer TMDC-ONB in dichloromethane (DCM) at 30 °C using DBU as a catalyst and mPEG (M_W = 2000 or 5000) as a macroinitiator. As shown in **Table 1**, the polycarbonate diblock copolymers P1 and P2 initiated by mPEGs of their M_Ws of 5000 and 2000, respectively, show M_n values of 10.2 kDa and 5.1 kDa, respectively. All polymers are featured by narrow polydispersity ($Đ$ = 1.10–1.13). The estimated degrees of polymerization show good agreements with calculated values using feed ratio and monomer conversion, indicating the ROPs undergo in living characteristics. The degree of polymerizations was calculated as 12 and 7, resulting from the comparison of the integral intensity of alkyne protons (δ = 2.62 ppm) with that of PEG protons (δ = 3.63 ppm) from ^{1}H NMR (Figure 1). The ^{1}H NMR and GPC analyses show that the targeted diblock polycarbonate polymers were successfully

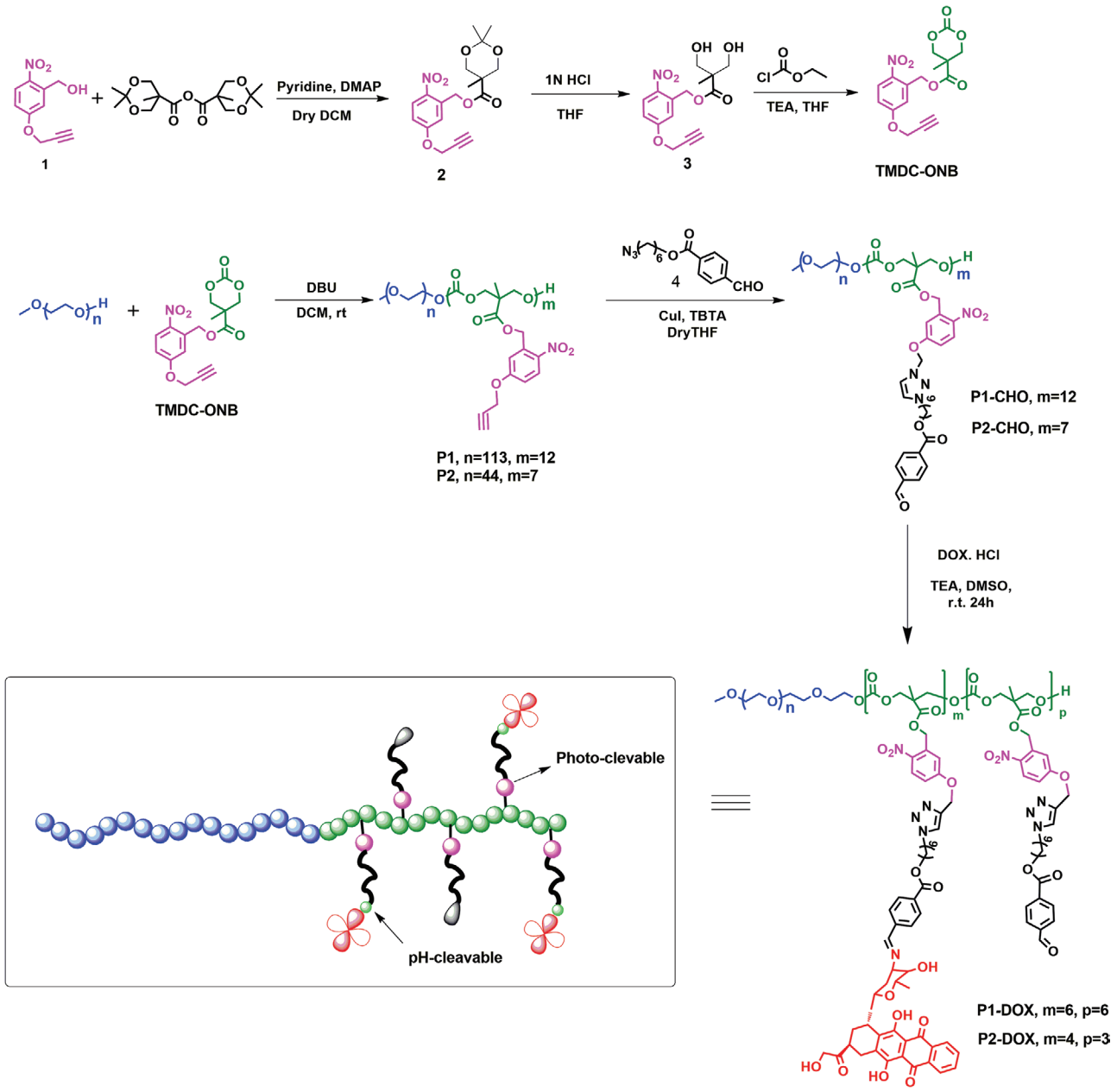

Scheme 1. Synthesis of TMDC-ONB monomer and polycarbonate prodrug polymers P1–DOX and P2–DOX.

Table 1. Properties of amphiphilic polycarbonate block copolymers and DOX contents of prodrug NMs.

Samples	M_n, NMR[a] [g mol^{-1}]	M_n, GPC[b] [g mol^{-1}]	$Đ$[b]	Diameter[c] [nm]	Diameter[d] [nm]	Theoretical DOX content [wt%]	Experimental DOX content[e] [wt%]
P1	9200	10 200	1.10				
P2	4500	5100	1.13				
P1–DOX	15 900	18 000	1.13	28	20 ± 2.5	16.2	14.0
P2–DOX	8700	10 000	1.15	35	23 ± 3.4	13.3	8.5

[a]Number average M_W estimated by ^{1}H NMR spectra; [b]Estimated by GPC with THF as eluent and polystyrene as standard; [c]Average diameter of NMs determined by DLS; [d]Average diameter of NMs determined by TEM; [e]Determined by UV–vis spectrometer.

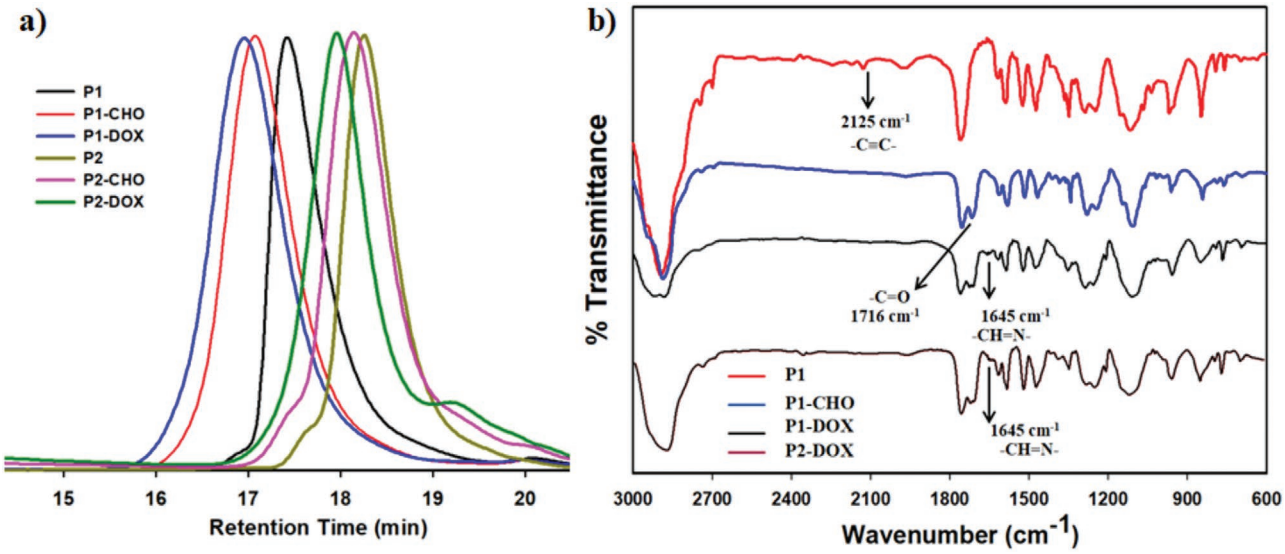

Figure 2. a) Overlay of GPC chromatograms of P1 and P2, P1–CHO and P2–CHO, and P1–DOX and P2–DOX and b) FTIR spectra of P1, P1–CHO, P1–DOX, and P2–DOX.

synthesized (Figure 1 and Figures S13 and S14, Supporting Information). The GPC chromatograms (**Figure 2**a) of P1 and P2 produced by the ROPs of TMDC-ONB using mPEG initiators of their M_W of 5000 and 2000, respectively, are characterized by unimodal and narrow polydispersity. P1 and P2 bearing pendant alkyne groups were modified to have aldehyde functionalities by using Cu(I)I/TBTA catalyzed azide–alkyne click reaction.[56] Small molecule 6-azidohexyl 4-formylbenzoate functionalized with azide and benzyl aldehyde was synthesized by the reported procedure[23] (see Figures S11 and S12, Supporting Information). The conversion of the click reactions was observed as indicated by the disappearance of alkyne protons peak at 2.62 ppm and presence of triazole protons peak at 7.74 ppm and aldehyde protons peak at 10.06 ppm in the ^{1}H NMR spectrum (Figure 1). As shown in Figure 2a, GPC curves of polymers P1–CHO and P2–CHO are similar to those of P1 and P2, respectively, with shifts to higher molecular weights from the corresponding precursor polymers, confirming the successful click functionalization. As illustrated in Scheme 1, the resultant aldehyde-functionalized polymers were further conjugated with DOX by the acid-sensitive Schiff base linkage in DMSO. In this reaction, 2 equiv of TEA was added to neutralize DOX·HCl and the amine groups in DOX were activated for the reaction. The chemical structures of the DOX conjugated polymers P1–DOX and P2–DOX were verified by ^{1}H NMR spectra (Figure 1 and Figure S15, Supporting Information). DOX conjugations to P1–CHO and P2–CHO were also characterized by GPC. After the conjugation of the DOX to the polymer, the peak intensities of aldehyde groups were decreased significantly in ^{1}H NMR and there are six and three aldehyde groups were free in P1–CHO and P2–CHO, respectively, corresponding to graft ratio of 50% and 43%, respectively. The partial conjugations of DOX to the two polymers might be due to the reversible Schiff-base formation, steric hindrance rendered by adjacent DOX and aldehyde benzene ring, and hydrogen bonding between aldehyde groups.[57]

A UV-Vis spectroscopy was used to confirm the successful preparation of the prodrug polymers. UV–vis absorption spectrum (Figure S16, Supporting Information) of P1–DOX shows 10 nm red shift compared with free DOX·HCl in water due to the fact that the conjugation of the DOX to the polymer backbone with Schiff base linkage results in change of the original structure of DOX·HCl. The resultant DOX contents of P1–DOX and P2–DOX was determined as 14.0% and 8.5%, respectively, as summarized in Table 1, from which we can conclude that the DOX content for P1–DOX is higher than P2–DOX. The theoretical DOX content is somewhat higher because the M_n values measured by GPC higher than those by ^{1}H NMR. IR spectra of P1–DOX and P2–DOX (Figure 2b) clearly show absorption peak assigned to imine (−C=N−) stretching frequency at 1645 cm^{-1} confirmed the successful conjugation of the DOX to the polymer.

3.2. Self-Assembly of the Polymer Prodrugs P1–DOX and P2–DOX

P1–DOX and P2–DOX polymers are expected to show amphiphilic nature because they are consisting of PEG and polycarbonate blocks. Thus, they can form NMs by the self-assembly in water by forming hydrophilic PEG corona and hydrophobic DOX-conjugated polycarbonate core. For the self-assembly aqueous solutions of the polymers were prepared by organic co-solvent method. Water was slowly added to the polymers dissolved in THF to induce the formation of aggregates, and the mixture was dialyzed against water to remove THF. The resultant aqueous solutions of polymers were analyzed by using DLS. The average size of NMs fabricated by P1–DOX and P2–DOX was 28 and 35 nm, respectively (**Figure 3**a,b inset). The TEM images of the NMs demonstrate that they are spherical aggregates (Figure 3a,b). The average diameter of 40 particles as measured from TEM images fabricated by P1–DOX and P2–DOX is about 20 ± 2.5 and 23 ± 3.4 nm,

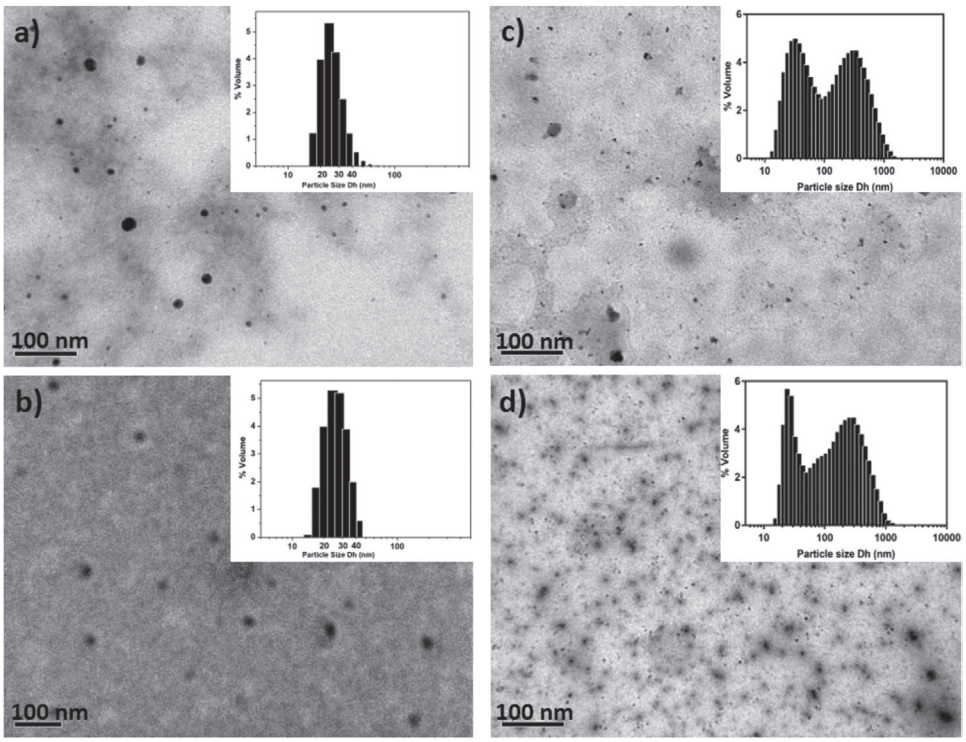

Figure 3. TEM images of NMs fabricated by a) P1–DOX and b) P2–DOX before UV irradiation and c) P1-DOX and d) P2-DOX after 60 min UV irradiation. Insets are the corresponding DLS histograms recorded with 0.1 wt% aqueous solutions of polymers using DLS.

respectively. The average sizes of the NMs measured by the TEM were about 10 nm smaller than that measured by DLS in the hydrated state of NMs. The critical micelle concentration (CMC) for P1 and P2 were determined by using Nile Red as a fluorescent probe. The CMC values for P1 and P2 were found to be 5.0×10^{-5} and 3.1×10^{-5} mol L^{-1}, respectively, from plots of fluorescence intensity versus log(concentration) (Figure S17, Supporting Information). The morphology of the NMs was investigated after the photocleavage of ONB ester using TEM. As showed in Figure 3c,d, upon 60 min UV light irradiation, most of the spherical micellar nanoparticles are disrupted to form irregular-shaped aggregates. This observation is mainly due to the fact that nitrobenzyl ester cleavage from the polymer form the hydrophilic carboxylic acid that leads to the change in the hydrophilic-hydrophobic balance. The size change of NMs after the UV light irradiation was monitored using DLS. As shown in in Figure 3c,d (inset), the average size of the NMs was increased to 500 nm. This could be attributed to the suspension of hydrophobic insoluble particles in the solution after the degradation of the polymer.

3.3. Photo-Cleavage Experiments

P1 and P2 were subjected to the photo-cleavage tests, since the ONB groups in the polymers are photo-cleaved to the corresponding *o*-nitrasobenzaldehyde to release free carboxylic acid upon irradiation with UV light (Figure S20, Supporting Information). The aqueous solutions of P1, P2, P1-DOX, and P2-DOX (0.2 mg mL^{-1}) were irradiated at 365 nm and absorption spectra were monitored at different time intervals (**Figure 4**). The absorbance band assigned to the ONB group at 305 nm decreases and the peak at 350 nm increases accordingly. No further change is observed after 1 h UV irradiation. In addition, there were clear visible color changes of the solution, from colorless to pale brown, confirming the formation of *o*-nitroso compound.

The photo-cleavage of ONB groups was further verified by using ^{1}H NMR spectra. **Figure 5**a shows ^{1}H NMR spectra of polymer P1 recorded after irradiation at different intervals. The area of the peak corresponding the benzylic protons at $\delta = 5.51$ ppm corresponding to ONB group decreases from 12 to 7.34 by 1 h of irradiation, confirming the photo-cleavage of ONB ester photon transfer radical mechanism. In addition, the photo-cleavage of ONB groups was further supported by GPC analysis. The irradiated polymer P1 for 1 h show a bimodal distribution in GPC chromatogram due to the cleavage of ONB ester (Figure 5b).

3.4. Photo-Controlled DOX-Release

The release of DOX from the NMs fabricated by the prodrug polymers, P1–DOX and P2–DOX, were investigated under the UV light irradiation. Micellar solutions of the polymer P1–DOX and P2–DOX prepared by the solvent exchange method were subjected to irradiate and the controlled release of DOX was monitored using fluorescence emission spectra at different irradiation intervals. **Figure 6** shows that the fluorescence emission intensity decrease gradually with increasing irradiation time,

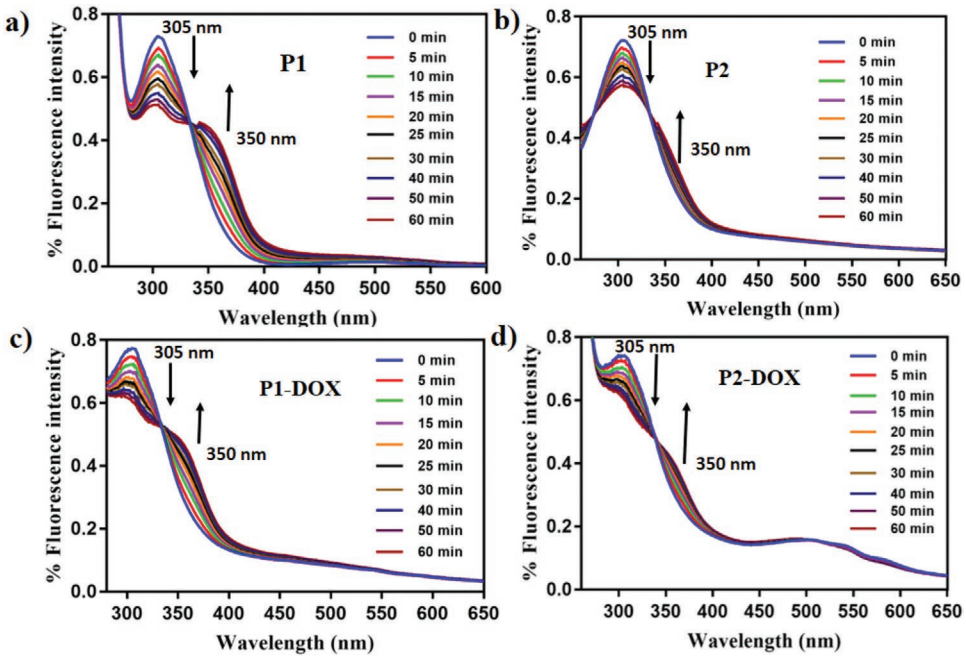

Figure 4. UV–vis spectral variations of 0.02 wt% aqueous solutions of a) P1, b) P2, c) P1-DOX, and d) P2-DOX recorded after irradiation at 365 nm at various intervals.

suggesting the cleavage of ONB ester groups and the release of DOX from the NMs into the aqueous environment. The DOX-release from P1–DOX and P2–DOX NMs was estimated as 72% and 83%, respectively, during 60 min of irradiation (Figure S18, Supporting Information). This observation mainly comes from the cleavage of the ONB groups, which results in hydrophobic-hydrophilic imbalance due to the formation of side chains of carboxylic acid. Aqueous P1-DOX and P2-DOX samples prepared without exposing to UV light show negligible changes in the emission intensity of DOX (Figure 6). Furthermore, the released DOX in pure water shows negligible change in emission intensity after 1 h UV irradiation, suggesting that the release of DOX from NMs was not due to the photo-bleaching of DOX (Figure S19, Supporting Information).

3.5. In Vitro Release of DOX

The in vitro DOX-releases from P1–DOX and P2–DOX NMs were investigated under different pH buffer media conditions:, that is, pH 7.4, pH 6.0, and pH 5.0 at 37 °C. The release study was performed for 72 h and the release profiles were constructed by measuring the released DOX fluorescence under excitation at 480 nm and emission at 550 nm. As shown in **Figure 7**, the

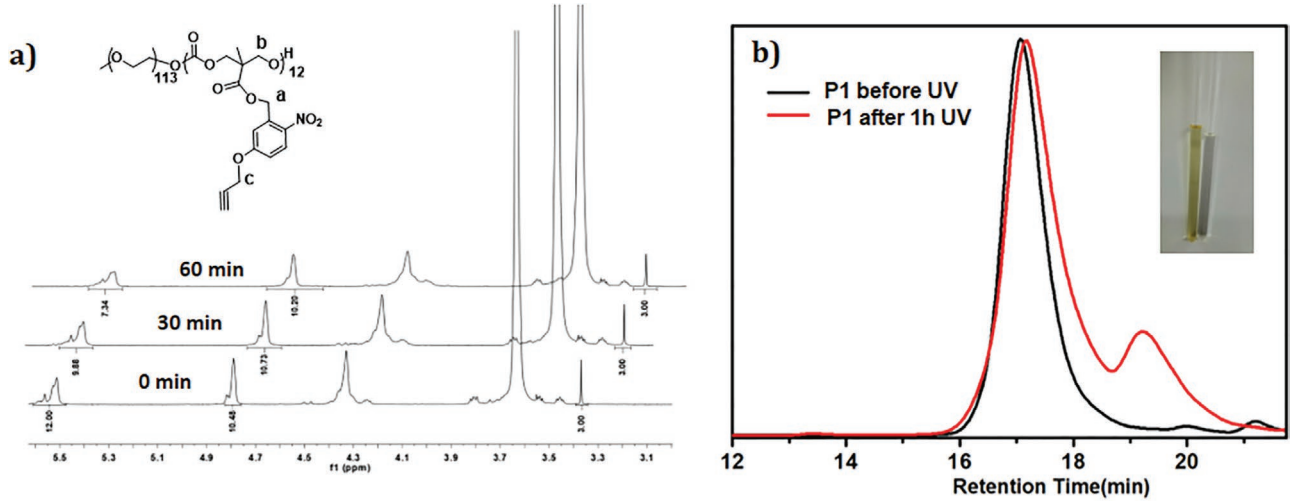

Figure 5. a) ^{1}H NMR spectra of P1 irradiated at 365 nm at different irradiation intervals and b) GPC chromatograms of P1 before and after 1 h of irradiation.

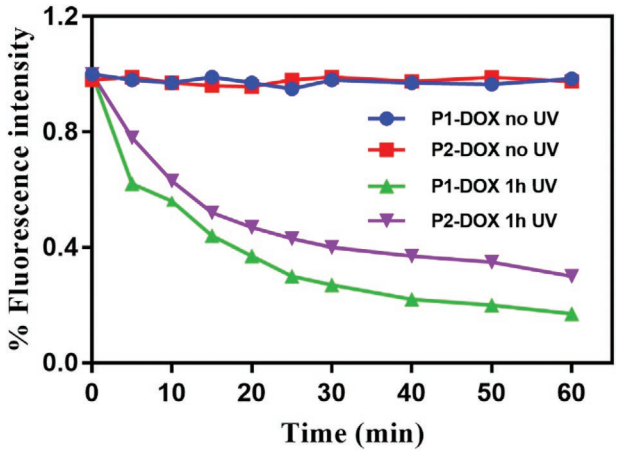

Figure 6. Photo-controlled DOX-release profiles of the P1–DOX and P2–DOX with and without UV light irradiation at different time intervals.

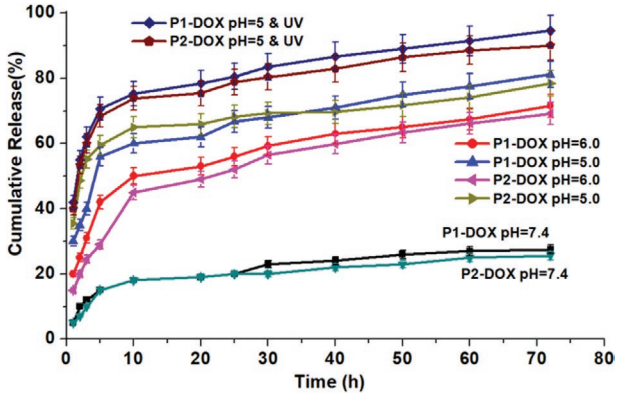

Figure 7. In vitro DOX-release profiles from P1–DOX and P2–DOX NMs at pH 7.4, pH 6. 0, pH 5.0, and pH 5.0 with 10 min UV light irradiation.

DOX-release from P1–DOX and P2–DOX NMs at pH 5.0 was much faster than at pH 6.0. For example, the DOX-release for P1–DOX and P2–DOX NMs at pH 5.0 is 81.2% and 78.5%, respectively, while the DOX-release is 71.2% and 69.2%, respectively, at pH 6.0. The DOX-release is only 27.5% and 25.6%, respectively, at pH 7.4. These results clearly indicate that the NMs are stable at physiological conditions, but release DOX at tumorous microenvironment (say, pH 5.0). This interesting pH-responsive DOX-release behavior is attributed to the cleavage of acid-sensitive imine linkages holding DOX molecules.

Inspired by the photo- and pH-responsive capability of P1–DOX and P2–DOX NMs, attempts were made to explore the simultaneous effect of both stimuli. The micellar solutions of P1–DOX and P2–DOX were agitated at pH 5 for 3 h at room temperature and then irradiated for 10 min so that both stimuli were in force. As shown in Figure 7, the DOX-release further increases to 70% and 68.5%, respectively, within 5 h, compared to 56% and 59.5%, respectively, obtained in the absence of irradiation. The release rate of DOX from nanoparticles increases significantly under the combined force of both pH- and photo-stimulus.

3.6. Cellular Viability

In order to evaluate the effect of P1–DOX and P2–DOX on cellular viability, Hisense WST-1 cell proliferation assays were performed. As shown in **Figure 8**a, the viability of CT-26 cells decreases with increasing of the concentration of nanoparticles. The cellular viability of the sample treated with P1–DOX show lower than that treated with P2–DOX at the same concentration, possibly due to the differences of the DOX content in P1–DOX and P2–DOX. The half-maximal inhibitory concentration (IC_{50}) for P1–DOX and P2–DOX was 0.034 ± 1.11 mg mL^{-1} and 0.28 ± 1.11 mg mL^{-1}, respectively (Figure 8b). These results suggest that the faster release of DOX from both P1–DOX and P2–DOX triggered by the endosomal pH causes the decrease in the cell viability.

3.7. Cellular Uptake

In order to confirm the intracellular uptake and the DOX-release from P1–DOX NMs, confocal microscopy was used. As illustrated in **Figure 9**a, following 6 h of incubation, the free DOX-incubated cells show strong red-fluorescence at nuclei of the cells while the cells incubated with P1–DOX NMs show red fluorescence in the cytoplasm due to the rapid internalization

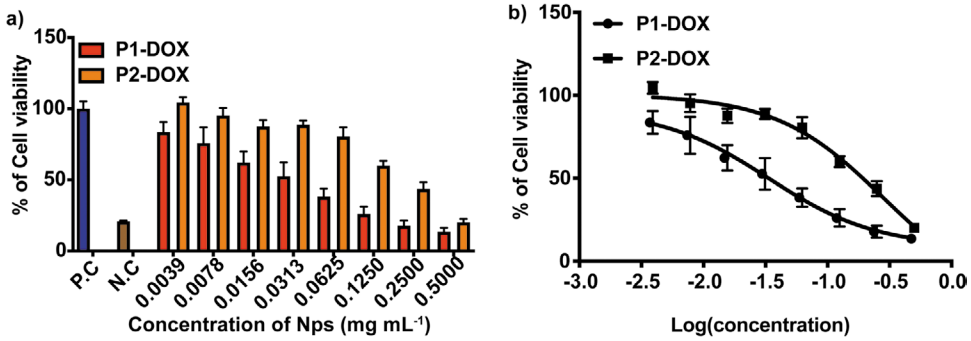

Figure 8. a) Cellular viability and b) IC_{50} curve of micellar solutions of P1–DOX and P2–DOX in varying NMs concentration. P.C = positive control (Cells only) and N.C = negative control (0.1% Triton X-100). $n = 3$.

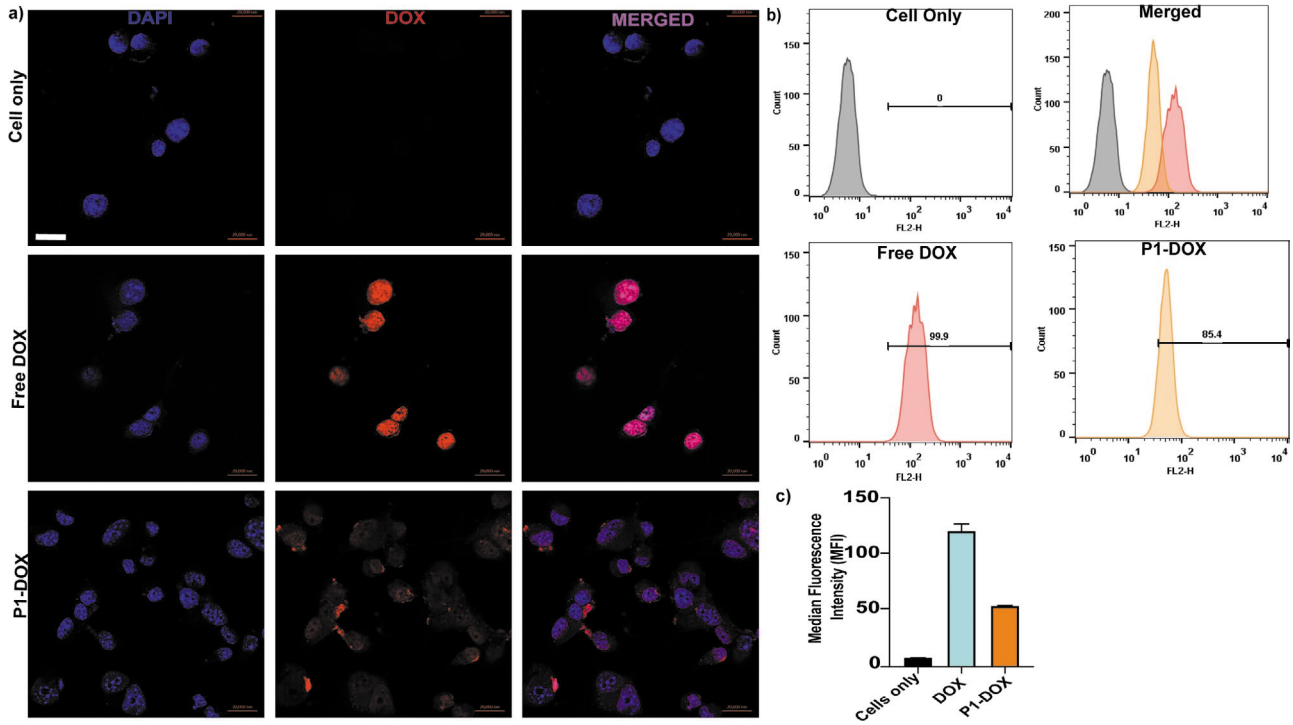

Figure 9. Cellular uptake profiles of P1–DOX: a) confocal microscopy images, b) FACS analysis, and c) intracellular mean fluorescence intensity after incubating with free DOX and P1–DOX NMs for 6 h. $n = 3$ and scale bar = 20 μm.

followed by the release of DOX that triggered by the endosomal pH. Since DOX is a small molecule, it can be easily diffused into cells and transported into nucleus. On the other hand, the P1–DOX NMs are internalized through endocytic pathway and then they release DOX at pH-triggered conditions.[58] These results demonstrate that the P1–DOX NMs are efficiently internalized into cancer cells via endocytosis and the pH-responsive capability the P1–DOX NMs enables the effective cytosolic release of DOX due to breakage of acid-sensitive Schiff's base linkage between the PEG and DOX.

4. Conclusions

Combining the ROP of newly designed carbonate monomer, PEGylation, azide-alkyne Huisgen cycloaddition and Schiff base reaction, two amphiphilic diblock polycarbonates covalently conjugated with DOX molecules on the side chains were prepared. Since the resultant polymers bear photo-sensitive ONB groups and acid-cleavable Schiff base linkages, they show photo- and pH-dual-stimuli-responsive feature. The polymer prodrugs, P1–DOX and P2–DOX, were self-assembled into spherical NMs of about 30 nm in size in aqueous solution. Stimuli-responsive DOX-release tests from the NMs were studied by applying photo/pH dual-stimuli individually to establish their effectiveness and drug release rates. Both stimuli were also applied simultaneously for the tenability of the drug release rates. In vitro studies demonstrated that the DOX-conjugated polymer NMs were efficiently internalized via endocytosis and the acid-labile Schiff's base linkages connecting DOX molecules with polymer enabled the cytosolic delivery of DOX. The DOX-conjugated polymer with photo- and pH- dual-stimuli responses can be a promising nanovehicle for the controlled release of drugs.

Supporting Information

Supporting Information is available from the Wiley Online Library or from the author.

Acknowledgements

N.K. and S.U. contributed equally to this work. This work was supported by the Basic Science Research Program through the National Research Foundation of Korea (2018R1D1A1A09081809 and 2019M3E5D1A02068082) and Korea Health Technology R&D Project, Ministry of Health and Welfare (HI17C1635).

Conflict of Interest

The authors declare no conflict of interest.

Keywords

block copolymers, drug delivery, ring-opening polymerizations, stimuli-responsive polymers

Received: April 7, 2020
Revised: May 18, 2020
Published online:

[1] M. E. Fox, F. C. Szoka, J. M. J. Fréchet, *Acc. Chem. Res.* **2009**, *42*, 1141.
[2] H. Gheybi, M. Adeli, *Polym. Chem.* **2015**, *6*, 2580.
[3] Y. Bae, S. Fukushima, A. Harada, K. Kataoka, *Angew. Chem., Int. Ed.* **2003**, *42*, 4640.
[4] H. Cabral, Y. Matsumoto, K. Mizuno, Q. Chen, M. Murakami, M. Kimura, Y. Terada, M. R. Kano, K. Miyazono, M. Uesaka, N. Nishiyama, K. Kataoka, *Nat. Nanotechnol.* **2011**, *6*, 815.
[5] G. Kocak, C. Tuncer, V. Bütün, *Polym. Chem.* **2017**, *8*, 144.
[6] M. H. Stenzel, *Chem. Commun.* **2008**, *2008*, 3486.
[7] Z. Xu, S. Liu, Y. Kang, M. Wang, *ACS Biomater. Sci. Eng.* **2015**, *1*, 585.
[8] Z. Xu, S. Liu, H. Liu, C. Yang, Y. Kang, M. Wang, *Chem. Commun.* **2015**, *51*, 15768.
[9] Y. Wang, N. Shen, K. Sakurai, Z. Tang, *Macromol. Biosci.* **2019**, *19*, 1900329.
[10] I. I. Slowing, B. G. Trewyn, S. Giri, V. S.-Y. Lin, *Adv. Funct. Mater.* **2007**, *17*, 1225.
[11] M. Liong, J. Lu, M. Kovochich, T. Xia, S. G. Ruehm, A. E. Nel, F. Tamanoi, J. I. Zink, *Nano Lett.* **2008**, *2*, 889.
[12] L. Zeng, Y. Li, T. Li, W. Cao, Y. Yi, W. Geng, Z. Sun, H. Xu, *Chem.–Asian J.* **2014**, *9*, 2295.
[13] M. K. Yu, Y. Y. Jeong, J. Park, S. Park, J. W. Kim, J. J. Min, K. Kim, S. Jon, *Angew. Chem., Int. Ed.* **2008**, *47*, 5362.
[14] Z. Xu, S. Liu, Y. Kang, M. Wang, *Nanoscale* **2015**, *7*, 5859.
[15] S.-M. Lee, S. T. Nguyen, *Macromolecules* **2013**, *46*, 9169.
[16] W. T. Al-Jamal, K. Kostarelos, *Acc. Chem. Res.* **2011**, *44*, 1094.
[17] U. Boas, P. M. H. Heegaard, *Chem. Soc. Rev.* **2004**, *33*, 43.
[18] X. Ma, Z. Zhou, E. Jin, Q. Sun, B. Zhang, J. Tang, Y. Shen, *Macromolecules* **2013**, *46*, 37.
[19] H.-T. Chen, M. F. Neerman, A. R. Parrish, E. E. Simanek, *J. Am. Chem. Soc.* **2004**, *126*, 10044.
[20] S. Shao, Q. Zhou, J. Si, J. Tang, X. Liu, M. Wang, J. Gao, K. Wang, R. Xu, Y. Shen, *Nat. Biomed. Eng.* **2017**, *1*, 745.
[21] X. Ke, D. J. Coady, C. Yang, A. C. Engler, J. L. Hedrick, Y. Y. Yang, *Polym. Chem.* **2014**, *5*, 2621.
[22] Y. Yu, C.-K. Chen, W.-C. Law, H. Sun, P. N. Prasad, C. Cheng, *Polym. Chem.* **2015**, *6*, 953.
[23] Y. Yu, C.-K. Chen, W.-C. Law, E. Weinheimer, S. Sengupta, P. N. Prasad, C. Cheng, *Biomacromolecules* **2014**, *15*, 524.
[24] S.-W. Wang, Y.-K. Lin, J.-Y. Fang, R.-S. Lee, *RSC Adv.* **2018**, *8*, 29321.
[25] D. Cao, J. He, J. Xu, M. Zhang, L. Zhao, G. Duan, Y. Cao, R. Zhou, P. Ni, *Polym. Chem.* **2016**, *7*, 4198.
[26] M. N. Ganivada, P. Kumar, P. Kanjilal, H. Dinda, J. D. Sarma, R. Shunmugam, *Polym. Chem.* **2016**, *7*, 4237.
[27] D. Li, Y. Song, J. He, M. Zhang, P. Ni, *ACS Biomater. Sci. Eng.* **2019**, *5*, 2307.
[28] X. Shi, M. Hou, S. Bai, X. Ma, Y.-E. Gao, B. Xiao, P. Xue, Y. Kang, Z. Xu, C. M. Li, *Mol. Pharmaceutics* **2017**, *14*, 4032.
[29] J. Liao, H. Zheng, Z. Fei, B. Lu, H. Zheng, D. Li, X. Xiong, Y. Yi, *Int. J. Biol. Macromol.* **2018**, *113*, 737.
[30] H. Horo, S. Das, B. Mandal, L. M. Kundu, *Int. J. Biol. Macromol.* **2019**, *121*, 1070.
[31] M. L. Adams, A. Lavasanifar, G. S. Kwon, *J. Pharm. Sci.* **2003**, *92*, 1343.
[32] H. Cabral, K. Miyata, K. Osada, K. Kataoka, *Chem. Rev.* **2018**, *118*, 6844.
[33] C. Li, S. Wallace, *Adv. Drug Delivery Rev.* **2008**, *60*, 886.
[34] X. Guo, L. Wang, X. Wei, S. Zhou, *J. Polym. Sci., Part A: Polym. Chem.* **2016**, *54*, 3525.
[35] J. Ding, D. Li, X. Zhuang, X. Chen, *Macromol. Biosci.* **2013**, *13*, 1300.
[36] H. Shen, Y. Xia, Z. Qin, J. Wu, L. Zhang, Y. Lu, X. Xia, W. Xu, *J. Polym. Sci., Part A: Polym. Chem.* **2017**, *55*, 2770.
[37] J. Sun, D. Jung, T. Schoppa, J. Anderski, M.-T. Picker, Y. Ren, D. Mulac, N. Stein, K. Langer, D. Kuckling, *ACS Appl. Bio Mater.* **2019**, *2*, 3038.
[38] J. Sun, W. Birnbaum, J. Anderski, M.-T. Picker, D. Mulac, K. Langer, D. Kuckling, *Biomacromolecules.* **2018**, *19*, 4677.
[39] J. Xuan, D. Han, H. Xia, Y. Zhao, *Langmuir* **2014**, *30*, 410.
[40] N. Kalva, N. Parekh, A. V. Ambade, *Polym. Chem.* **2015**, *6*, 6826.
[41] F. Yang, Z. Cao, G. Wang, *Polym. Chem.* **2015**, *6*, 7995.
[42] O. Bertrand, J.-F. Gohy, *Polym. Chem.* **2017**, *8*, 52.
[43] D. Hu, Y. Li, Y. Niu, L. Li, J. He, X. Liu, X. Xia, Y. Lu, Y. Xiong, W. Xu, *RSC Adv.* **2014**, *4*, 47929.
[44] G. Rokicki, *Prog. Polym. Sci.* **2000**, *25*, 259.
[45] S. Tempelaar, L. Mespouille, O. Coulembier, P. Dubois, A. P. Dove, *Chem. Soc. Rev.* **2013**, *42*, 1312.
[46] G. Becker, F. R. Wurm, *Chem. Soc. Rev.* **2018**, *47*, 7739.
[47] A. P. Dove, *ACS Macro Lett.* **2012**, *1*, 1409.
[48] N. E. Kamber, W. Jeong, R. M. Waymouth, R. C. Pratt, B. G. G. Lohmeijer, J. L. Hedrick, *Chem. Rev.* **2007**, *107*, 5813.
[49] Y. Dai, X. Zhang, *Polym. Chem.* **2017**, *8*, 7429.
[50] D. Hu, H. Peng, Y. Niu, Y. Li, Y. Xia, L. Li, J. He, X. Liu, X. Xia, Y. Lu, W. Xu, *J. Polym. Sci., Part A: Polym. Chem.* **2015**, *53*, 750.
[51] J. Y. Teo, W. Chin, X. Ke, S. Gao, S. Liu, W. Cheng, J. L. Hedrick, Y. Y. Yang, *Nanomed.: Nanotechnol., Biol. Med.* **2017**, *13*, 431.
[52] M. Xie, L. Yu, Z. Li, Z. Zheng, X. Wang, *J. Polym. Sci., Part A: Polym. Chem.* **2016**, *54*, 3583.
[53] J.-M. Schumers, J.-F. Gohy, C.-A. Fustin, *Polym. Chem.* **2010**, *1*, 161.
[54] T. Magbitang, V. Y. Lee, J. N. Cha, H.-L. Wang, W. R. Chung, R. D. Miller, G. Dubois, W. Volksen, H.-C. Kim, J. L. Hedrick, *Angew. Chem., Int. Ed.* **2005**, *44*, 7574.
[55] B. Vonhoeren, S. Dalgleish, L. Hu, M. M. Matsushita, K. Awaga, B. J. Ravoo, *ACS Appl. Mater. Interfaces* **2015**, *7*, 7049.
[56] N. G. Patil, R. Augustine, Y. Zhang, S. C. Hong, I. Kim, *ACS Omega* **2019**, *4*, 6660.
[57] S. Q. Liu, Y. W. Tong, Y.-Y. Yang, *Biomaterials* **2005**, *26*, 5064.
[58] J. Wang, Y. Lu, S. T. Li, X. Wang, Y. Huang, R. P. Tang, *Mater. Sci. Eng., C* **2019**, *94*, 169.